



IUCrData

ISSN 2414-3146

2-{1-[(6*R,S*)-3,5,5,6,8,8-Hexamethyl-5,6,7,8-tetrahydronaphthalen-2-yl]ethylidene}-*N*-methylhydrazinecarbothioamide

Ana Paula Lopes de Melo,^a Alex Fabiani Claro Flores,^a Leandro Bresolin,^{a*} Bárbara Tirloni^b and Adriano Bof de Oliveira^c

Received 24 November 2023

Accepted 26 November 2023

Edited by M. Bolte, Goethe-Universität Frankfurt, Germany

Keywords: thiosemicarbazone; fixolide thiosemicarbazone; chiral thiosemicarbazone; hydrogen-bonded ribbon; fixolide derivative; crystal structure.

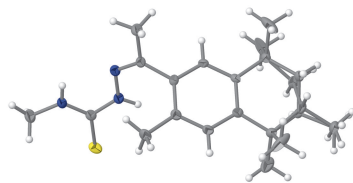
CCDC reference: 2302507

Structural data: full structural data are available from iucrdata.iucr.org

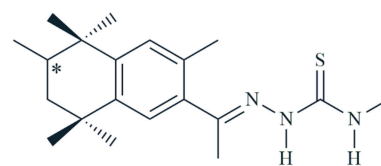
^aEscola de Química e Alimentos, Universidade Federal do Rio Grande, Av. Itália km 08, Campus Carreiros, 96203-900 Rio Grande-RS, Brazil, ^bDepartamento de Química, Universidade Federal de Santa Maria, Av. Roraima 1000, Campus Universitário, 97105-900 Santa Maria-RS, Brazil, and ^cDepartamento de Química, Universidade Federal de Sergipe, Av. Marcelo Deda Chagas s/n, Campus Universitário, 49107-230 São Cristóvão-SE, Brazil. *Correspondence e-mail: leandro_bresolin@yahoo.com.br

The reaction between a racemic mixture of (*R,S*)-fixolide and 4-methylthiosemicarbazide in ethanol with a 1:1 stoichiometric ratio and catalysed with HCl, yielded the title compound, C₂₀H₃₁N₃S [common name: (*R,S*)-fixolide 4-methylthiosemicarbazone]. There is one crystallographically independent molecule in the asymmetric unit, which is disordered over the aliphatic ring [site-occupancy ratio = 0.667 (13):0.333 (13)]. The disorder includes the chiral C atom, the neighbouring methylene group and the methyl H atoms of the methyl group bonded to the chiral C atom. The maximum deviations from the mean plane through the disordered aliphatic ring amount to 0.328 (6) and −0.334 (6) Å [r.m.s.d. = 0.2061 Å], and −0.3677 (12) and 0.3380 (12) Å [r.m.s.d. = 0.2198 Å] for the two different sites. Both fragments show a half-chair conformation. Additionally, the N–N–C(=S)–N entity is approximately planar, with the maximum deviation from the mean plane through the selected atoms being 0.0135 (18) Å [r.m.s.d. = 0.0100 Å]. The molecule is not planar due to the dihedral angle between the thiosemicarbazone entity and the aromatic ring, which amounts to 51.8 (1)°, and due to the *sp*³-hybridized carbon atoms of the fixolide fragment. In the crystal, the molecules are connected by H···S interactions with graph-set motif C(4), forming a mono-periodic hydrogen-bonded ribbon along [100]. The Hirshfeld surface analysis suggests that the major contributions for the crystal cohesion are [(*R,S*)-isomers considered separately] H···H (75.7%), H···S/S···H (11.6%), H···C/C···H (8.3% and H···N/N···H (4.4% for both of them).

3D view



Chemical scheme



Published under a CC BY 4.0 licence

Structure description

The thiosemicarbazone chemistry is essentially interdisciplinary and these molecules, characterized by the $R_1R_2N-N(H)-C(=S)-NR_3R_4$ functional group, play an important role in a wide range of scientific disciplines, including biochemistry, coordination chemistry and materials science. Originally, thiosemicarbazone derivatives were the major product of a condensation reaction employed in the organic chemistry for the detection of ketones and aldehydes, using thiosemicarbazide as analytical reagent (Freund & Schander, 1902). As a result of the huge structural diversity of ketones and aldehydes, a large number of thiosemicarbazone derivatives can be easily obtained for various applications. One of the earliest reports on the application of the thiosemicarbazones can be traced back to the middle of the 1940s, when these compounds were proved to be effective on *Mycobacterium tuberculosis* growth inhibition (Domagk *et al.*, 1946). Until today, the biological activity of thiosemicarbazone derivatives remains one of the most important approaches for this chemistry. Thiosemicarbazone derivatives are well known for their biological properties, *e.g.*, antifungal (Bajaj *et al.*, 2021), antitumoural (Farias *et al.*, 2021; Rocha *et al.*, 2019; Siqueira *et al.*, 2019) and anti-inflammatory pathologies (Kanso *et al.*, 2021), to cite just a few examples. For instance, thiosemicarbazone coordination compounds also have applications in diagnostic medical imaging and theranostics (Dilworth & Hueting, 2012; Parrilha *et al.*, 2022). In addition, thiosemicarbazone complexes are employed as single-molecule precursors in the synthesis of nanostructured materials through thermal decomposition techniques. Thus, Co^{II} , Cd^{II} and Zn^{II} complexes are used for the synthesis of CoS and Co_9S_8 (Pawar & Garje, 2015), CdS (Pawar *et al.*, 2016) and ZnS (Palve & Garje, 2011) nanoparticles, respectively. For a review of the coordination chemistry of thiosemicarbazones, showing the different bonding modes with diverse metal centres and Lewis acidity, see: Lobana *et al.* (2009). Finally, thiosemicarbazone derivatives can act as organic corrosion inhibitors, *e.g.*, as a layer of protection for carbon steel AISI 1020 in a hydrochloric acid medium (Goulart *et al.*, 2013) and

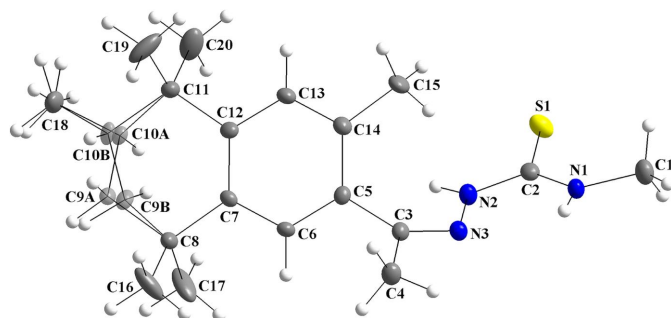


Figure 1
The molecular structure of the title compound, showing the atom labeling and displacement ellipsoids drawn at the 40% probability level. Disordered carbon atoms are drawn with 30% transparency and labelled C9A/C10A (*R*-isomer [s.o.f. = 0.667 (13)] and C9B/C10B for the (*S*)-isomer [s.o.f. = 0.333 (13)].

for a theoretical study of the corrosion inhibition concerning dimeric thiosemicarbazones, see: Silva & Martínez-Huitle (2021).

As part of our interest in this chemistry, we report herein the synthesis, crystal structure and Hirshfeld analysis of the title (*R,S*)-fixolide 4-methylthiosemicarbazone compound. The molecular structure matches the asymmetric unit, which is disordered over the aliphatic ring, with the site-occupancy ratio being 0.667 (13):0.333 (13) for the *A*- and *B*-labelled atoms, respectively (Fig. 1). A racemic mixture of fixolide was employed as starting material. As the disorder includes the C10 chiral centre, with C10A–H10A and C10B–HB bonds in opposite directions, (*R*)- and (*S*)-isomers are observed. The C9 atom was also split over two positions into C9A and C9B, with the same respective occupancy ratio. The C18 atom is itself not disordered, but the H atoms attached to the carbon atom of this methyl group were refined as disordered to get the best orientations for the C–H bonds, since it is bonded to the sp^3 -hybridized C10A and C10B atoms. The displacement ellipsoids for C16, C17, C19 and C20 are prolate-like, but no disorder was suggested by the data analysis.

The maximum deviations from the mean plane through the C7/C8/C9A/C10A/C11/C12 atoms amounts to 0.328 (6) Å for C9A and -0.334 (6) Å for C10A (r.m.s.d. = 0.2061 Å). The torsion angle for the C8/C9A/C10A/C11 atom chain is -65.3 (7)° and the aliphatic ring adopts a half-chair confor-

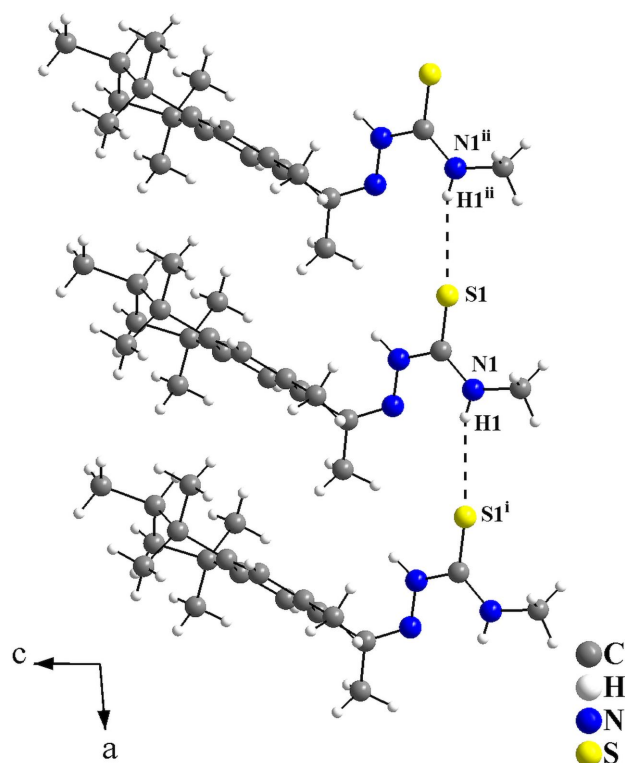


Figure 2
Graphical representation of the H...S intermolecular interactions for the title compound viewed along [010]. The interactions are drawn as dashed lines, with graph-set motif C(4), and connect the molecules into a mono-periodic hydrogen-bonded ribbon along [100]. Only the major occupied sites are drawn for clarity. [Symmetry codes: (i) $x + 1, y, z$; (ii) $x - 1, y, z$].

Table 1
Hydrogen-bond geometry (Å, °).

$D-H\cdots A$	$D-H$	$H\cdots A$	$D\cdots A$	$D-H\cdots A$
$N1-H1\cdots S1^i$	0.86	2.87	3.445 (3)	126

Symmetry code: (i) $x + 1, y, z$.

mation. Considering the $C7/C8/C9B/C10B/C11/C12$ entity, the deviations amount to -0.3677 (12) Å for $C9B$ and 0.3380 (12) Å for $C10B$ (r.m.s.d. = 0.2198 Å) and the torsion angle for the $C8/C9B/C10B/C11$ chain is 70.2 (14)°, which also resembles a half-chair conformation for the ring.

Concerning the thiosemicarbazone entity, the torsion angles for the $N3/N2/C2/N1$ and the $N3/N2/C2/S1$ atom chains amount to 1.2 (4) and -178.1 (2)°, respectively. The maximum deviation from the mean plane through the $N3/N2/C2/S1/N1$ atoms is 0.0135 (18) Å for $N2$ (r.m.s.d. = 0.0100 Å), thus, the fragment is approximately planar. The molecule of the title compound is not planar due to the sp^3 -hybridized C atoms of the apliphatic ring and due to the dihedral angle between the mean plane through the $N3/N2/C2/S1/N1$ atoms and the mean plane through the aromatic ring of the fixolide fragment, which amounts to 51.8 (1)°.

In the crystal, the molecules are connected by $N-H\cdots S$ interactions, with graph-set motif $C(4)$, forming a mono-periodic hydrogen-bonded ribbon along $[100]$ (Fig. 2, Table 1). The molecular arrangement resembles a zigzag or a herringbone motif when viewed along $[100]$ (Fig. 3).

The Hirshfeld surface analysis (Hirshfeld, 1977), the graphical representations and the two-dimensional Hirshfeld surface fingerprint plots for the title compound were performed using *CrystalExplorer* (Wolff *et al.*, 2012). The Hirshfeld surface analysis of the crystal structure indicates that the most relevant intermolecular interactions for crystal cohesion are $H\cdots H$ (75.7%), $H\cdots S/S\cdots H$ (11.6%), $H\cdots C/C\cdots H$ (8.3% and $H\cdots N/N\cdots H$ (4.4%). The graphics of the Hirshfeld surface of the title compound are represented with transparency in two opposite side-views and separate figures for clarity (Fig. 4). The locations of the strongest intermolecular contacts are indicated in red, *i.e.*, the regions around

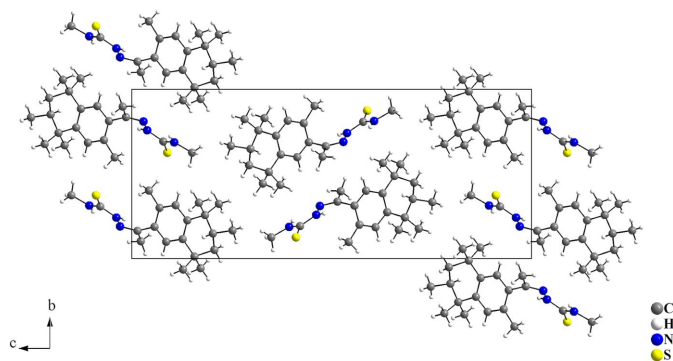


Figure 3
Section of the crystal packing of the title compound. The arrangement of the molecules shows a zigzag or a herringbone motif when viewed along $[100]$. Only the major occupied sites are drawn for clarity.

the $H1$ and $S1$ atoms. These atoms are those involved in the $H\cdots S$ interactions shown in a previous figure (Fig. 2) and in Table 1.

Although the Hirshfeld surface graphical representation shows, in red, locations of intermolecular contacts involving H atoms attached to C atoms, no $C-H\cdots H-C$ intermolecular interactions can be assigned. The fixolide fragment is a non-polar organic periphery and only weak intermolecular interactions, *e.g.*, London dispersion forces, can be considered. The contribution of $H\cdots H$ intermolecular interactions in the supramolecular arrangement of crystal structures has been studied (Almeida *et al.*, 2017), but this is not the focus of the present work. The crystal structure of the title compound is disordered, the H atoms were placed geometrically, the R -factor amounts to 0.079 and no additional experiment for the intermolecular interactions was performed, so it is not recommended to assure such contacts here. Additionally, no short $H\cdots H$ intermolecular distances were observed.

The contributions to the crystal packing are shown as two-dimensional Hirshfeld surface fingerprint plots with cyan dots (Fig. 5). The d_i (x -axis) and the d_e (y -axis) values are the closest internal and external distances from given points on the Hirshfeld surface (in Å).

To the best of our knowledge and from using database tools such as *SciFinder* (Chemical Abstracts Service, 2023) and the Cambridge Structural Database (CSD, accessed *via* WebCSD

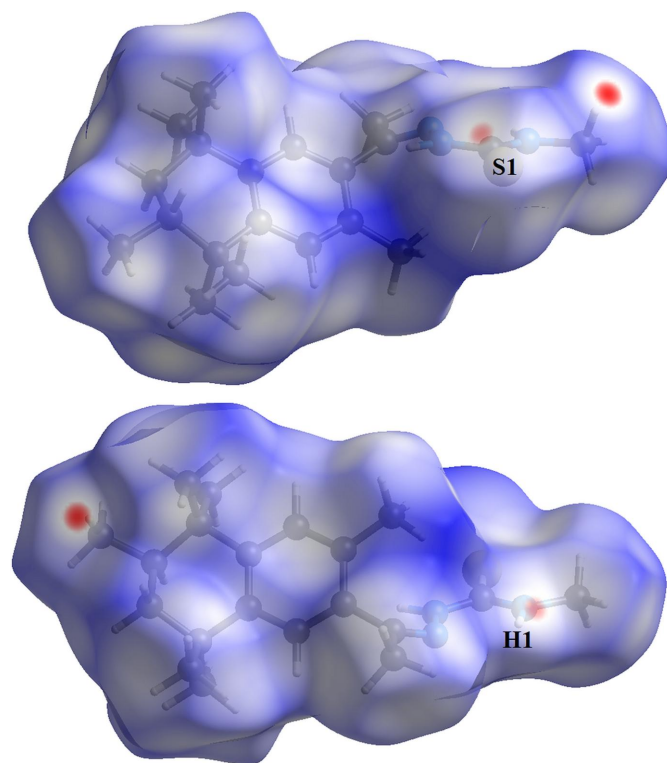


Figure 4
Two opposite side-views in separate figures of the Hirshfeld surface graphical representation (d_{norm}) for the title compound. The surface is drawn with transparency and simplified for clarity. The regions with strongest intermolecular interactions are shown in red. (d_{norm} range: -0.142 to 1.510 .)

Table 2

Selected torsion angles ($^{\circ}$) for the disordered fixolide 4-methylthiosemicarbazone and the fixolide carboxylic acid derivatives.

Compound	Isomer	Chiral atom (s.o.f.)	Atom chain	Torsion angle
$C_{20}H_{31}N_3S^a$	<i>R</i>	C10A [0.667 (13)]	C8–C9A–C10A–C11	–65.3 (7)
$C_{20}H_{31}N_3S^a$	<i>S</i>	C10B [0.333 (13)]	C8–C9B–C10B–C11	70.2 (14)
$C_{17}H_{24}O_2^b$	<i>R</i>	C10A [0.683 (4)]	C9–C10A–C11A–C12	–67.0 (3)
$C_{17}H_{24}O_2^b$	<i>S</i>	C10B [0.317 (4)]	C9–C10B–C11B–C12	71.8 (6)

Notes: (a) (*R,S*)-Fixolide 4-methylthiosemicarbazone, reported in this work (Fig. 1); (b) (*R,S*)-fixolide carboxylic acid derivative (Kuhlich *et al.*, 2010) (Fig. 7).

on November 18, 2023; Groom *et al.*, 2016), this work represents the first report on the synthesis, crystal structure and Hirshfeld analysis of the fixolide 4-methylthiosemicarbazone molecule. Thus, two crystal structures with similarities to the title compound were selected for comparison.

The first selected example is the crystal structure of the tetralone 4-ethylthiosemicarbazone (Oliveira *et al.*, 2017). There are two molecules with atoms in general positions forming the asymmetric unit, one of them being disordered over the ethyl fragment. In the crystal, the molecules are linked by $H \cdots S$ interactions along [100], with graph-set motif *C*(4), and forming a mono-periodic hydrogen-bonded ribbon (Fig. 6), as observed to the title compound (Fig. 2). The tetralone entity consists of one aliphatic and one aromatic ring, and for the non-polar organic periphery are suggested weak intermolecular interactions only, since even π – π interactions are not present in the structure.

The second example is the crystal structure of a (*R,S*)-fixolide carboxylic acid derivative (Kuhlich *et al.*, 2010). For

this structure, only one crystallographic independent molecule is observed in the asymmetric unit, which shows disorder over the aliphatic ring and two methyl groups (Fig. 7). The chiral centre is disordered, C10A and C10B, and two isomers are observed, namely the (*R*)- and (*S*)-forms. For the synthesis, a racemic mixture of fixolide was used as starting material. For the (*R,S*)-fixolide carboxylic acid derivative, the s.o.f. ratio amounts to 0.683 (4):0.317 (4). The torsion angles of the C9/C10A/C11A/C12 and the C9/C10B/C11B/C12 atom chains amount to -67.0 (3) and 71.8 (6) $^{\circ}$, respectively, being similar to the selected chains of the title compound (Table 2).

Synthesis and crystallization

The starting materials were commercially available and were used without further purification. The synthesis of the title

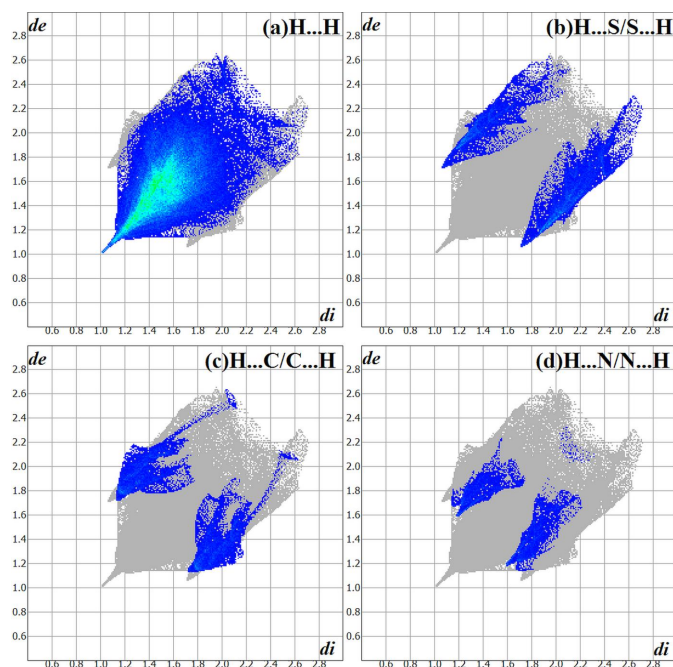


Figure 5

The Hirshfeld surface two-dimensional fingerprint plot for the title compound showing the (a) $H \cdots H$ (75.7%), (b) $H \cdots S/S \cdots H$ (11.6%), (c) $H \cdots C/C \cdots H$ (8.3%) and (d) $H \cdots N/N \cdots H$ (4.4%) contacts in detail (cyan dots) and the contributions of the interactions for the crystal packing. The d_i (x-axis) and the d_e (y-axis) values are the closest internal and external distances from given points on the Hirshfeld surface (in Å).

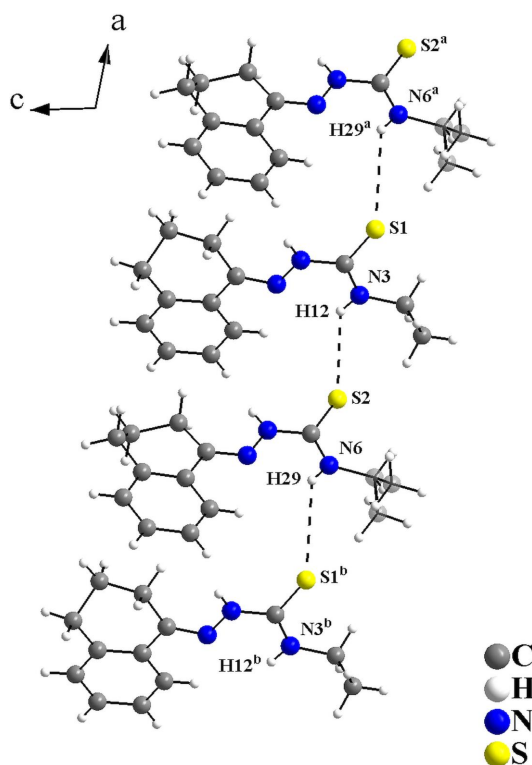


Figure 6

Graphical representation of the $H \cdots S$ intermolecular interactions for the tetralone 4-ethylthiosemicarbazone structure (Oliveira *et al.*, 2017) viewed along $[0\bar{1}0]$. The interactions are drawn as dashed lines and link the molecules along [100] with graph-set motif *C*(4), forming a mono-periodic hydrogen-bonded ribbon. Disordered atoms are drawn with 40% transparency. [Symmetry codes: (a) $x + 1, y, z$; (b) $x - 1, y, z$.]

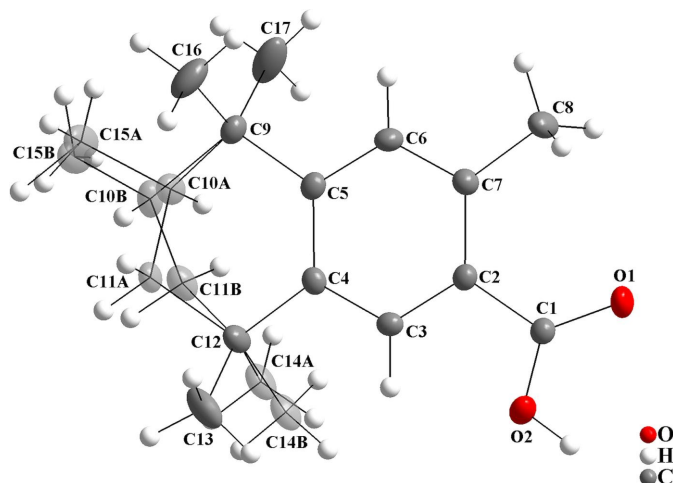


Figure 7

The molecular structure of the (*R,S*)-fixolide carboxylic acid derivative, showing the atom labelling and displacement ellipsoids drawn at the 40% probability level (Kuhlich *et al.*, 2010). Disordered atoms are drawn with 40% transparency and labelled C10A, C11A, C14A and C15A for the (*R*)-isomer [s.o.f. = 0.683 (4)] and C10B, C11B, C14B and C15B for the (*S*)-isomer [s.o.f. = 0.317 (4)].

compound was adapted from previously reported procedures (Freund & Schander, 1902; Oliveira *et al.*, 2017). A mixture of the racemic fixolide (5 mmol) and 4-methylthiosemicarbazide (5 mmol) in ethanol (80 ml), catalysed with HCl, was stirred and refluxed for 8 h. After cooling at room temperature, a colourless crystalline solid precipitated, was filtered off and washed with cold ethanol. The crystalline solid was dissolved in warm ethanol and single crystals suitable for X-ray diffraction were obtained by slow evaporation of the solvent at room temperature. The site-occupancy ratio of the disordered atoms refined to 0.667 (13):0.333 (13).

Refinement

Crystal data, data collection and structure refinement details are summarized in Table 3. The crystallographically independent molecule is disordered over the aliphatic ring (C9A, C9B, C10A and C10B) (Fig. 1). The s.o.f. for the *A*-labelled atoms amounts to 0.667 (13), while for the *B*-labelled atoms it is 0.333 (13). Although the displacement ellipsoids of C16, C17, C19 and C20 are prolate-like in comparison with the ellipsoids of other methyl groups, *e.g.*, C1, C4, C15 and C18, no additional disorder was indicated by the data analysis.

The hydrogen atoms attached to carbon and nitrogen atoms were positioned with idealized geometry and constrained to ride on their parent atoms. To get the best orientations for the C–H bonds of the C18H₃ group, which is bonded to the C10A and C10B atoms, the methyl hydrogen atoms were split into two positions, located geometrically and refined using a riding model [$U_{\text{iso}}(\text{H}) = 1.5U_{\text{eq}}(\text{C})$; C–H bonds lengths set to 0.96 Å]. The other methyl groups were allowed to rotate but not to tip to best fit the experimental electron density and the same C–H bond lengths value was set, also with $U_{\text{iso}}(\text{H}) = 1.5U_{\text{eq}}(\text{C})$. The $U_{\text{iso}}(\text{H}) = 1.2U_{\text{eq}}(\text{C})$ relation was employed for

Table 3

Experimental details.

Crystal data	
Chemical formula	C ₂₀ H ₃₁ N ₃ S
<i>M_r</i>	345.54
Crystal system, space group	Monoclinic, <i>P</i> 2 ₁ / <i>c</i>
Temperature (K)	100
<i>a</i> , <i>b</i> , <i>c</i> (Å)	5.867 (3), 11.790 (4), 27.983 (9)
β (°)	94.907 (14)
<i>V</i> (Å ³)	1928.7 (12)
<i>Z</i>	4
Radiation type	Mo <i>K</i> α
μ (mm ⁻¹)	0.17
Crystal size (mm)	0.21 × 0.20 × 0.15
Data collection	
Diffractometer	Bruker D8 Venture Photon 100 area detector diffractometer
Absorption correction	Multi-scan (<i>SADABS</i> ; Krause <i>et al.</i> , 2015)
<i>T_{min}</i> , <i>T_{max}</i>	0.690, 0.746
No. of measured, independent and observed [<i>I</i> > 2σ(<i>I</i>)] reflections	31284, 4822, 3250
<i>R_{int}</i>	0.092
(sin θ/λ) _{max} (Å ⁻¹)	0.668
Refinement	
<i>R</i> [<i>F</i> ² > 2σ(<i>F</i> ²)], <i>wR</i> (<i>F</i> ²), <i>S</i>	0.079, 0.201, 1.06
No. of reflections	4822
No. of parameters	243
H-atom treatment	H-atom parameters constrained
Δρ _{max} , Δρ _{min} (e Å ⁻³)	0.70, −0.43

Computer programs: *APEX3* and *SAINT* (Bruker, 2015), *SHELXT2014/5* (Sheldrick, 2015a), *SHELXL2018/3* (Sheldrick, 2015b), *DIAMOND* (Brandenburg, 2006), *Crystal-Explorer* (Wolff *et al.*, 2012), *WinGX* (Farrugia, 2012), *pubCIF* (Westrip, 2010) and *enCIFer* (Allen *et al.*, 2004).

the other C–H bonds and, for the phenyl ring H atoms, the C–H bond lengths were set to 0.93 Å. For the disordered –CH₂– fragment (C9A and C9B), the C–H bond-length value was set to 0.97 Å and for the disordered tertiary C atoms (C10A and C10B), the C–H bond lengths amount to 0.98 Å. Finally, the N–H bond lengths, with $U_{\text{iso}}(\text{H}) = 1.2U_{\text{eq}}(\text{N})$, were set to 0.86 Å.

Acknowledgements

APLM thanks CAPES for the award of a PhD scholarship. The authors thank the Department of Chemistry of the Federal University of Santa Maria/Brazil for the access to the X-ray diffraction facility.

Funding information

Funding for this research was provided by: Coordenação de Aperfeiçoamento de Pessoal de Nível Superior – Brazil (CAPES) – Finance Code 001.

References

- Allen, F. H., Johnson, O., Shields, G. P., Smith, B. R. & Towler, M. (2004). *J. Appl. Cryst.* **37**, 335–338.
- Almeida, L. R. de, Carvalho, P. S. Jr, Napolitano, H. B., Oliveira, S. S., Camargo, A. J., Figueredo, A. S., de Aquino, G. L. B. & Carvalho-Silva, V. H. (2017). *Cryst. Growth Des.* **17**, 5145–5153.

- Bajaj, K., Buchanan, R. M. & Grapperhaus, C. A. (2021). *J. Inorg. Biochem.* **225**, 111620.
- Brandenburg, K. (2006). *DIAMOND*. Crystal Impact GbR, Bonn, Germany.
- Bruker (2015). *APEX3* and *SAINT*. Bruker AXS Inc., Madison, Wisconsin, USA.
- Chemical Abstracts Service (2023). Columbus, Ohio, USA (accessed via SciFinder on November 18, 2023).
- Dilworth, J. R. & Hueting, R. (2012). *Inorg. Chim. Acta*, **389**, 3–15.
- Domagk, G., Behnisch, R., Mietzsch, F. & Schmidt, H. (1946). *Naturwissenschaften*, **33**, 315.
- Farias, R. L., Polez, A. M. R., Silva, D. E. S., Zanetti, R. D., Moreira, M. B., Batista, V. S., Reis, B. L., Nascimento-Júnior, N. M., Rocha, F. V., Lima, M. A., Oliveira, A. B., Ellena, J., Scarim, C. B., Zambom, C. R., Brito, L. D., Garrido, S. S., Melo, A. P. L., Bresolin, L., Tirloni, B., Pereira, J. C. M. & Netto, A. V. G. (2021). *Mater. Sci. Eng. C*, **121**, 111815.
- Farrugia, L. J. (2012). *J. Appl. Cryst.* **45**, 849–854.
- Freund, M. & Schander, A. (1902). *Ber. Dtsch. Chem. Ges.* **35**, 2602–2606.
- Goulart, C. M., Esteves-Souza, A., Martinez-Huitle, C. A., Rodrigues, C. J. F., Maciel, M. A. M. & Echevarria, A. (2013). *Corros. Sci.* **67**, 281–291.
- Groom, C. R., Bruno, I. J., Lightfoot, M. P. & Ward, S. C. (2016). *Acta Cryst.* **B72**, 171–179.
- Hirshfeld, H. L. (1977). *Theor. Chim. Acta*, **44**, 129–138.
- Kanso, F., Khalil, A., Nouredine, H. & El-Makhour, Y. (2021). *Int. Immunopharmacol.* **96**, 107778.
- Krause, L., Herbst-Irmer, R., Sheldrick, G. M. & Stalke, D. (2015). *J. Appl. Cryst.* **48**, 3–10.
- Kuhlich, P., Göstl, R., Metzinger, R., Piechotta, C. & Nehls, I. (2010). *Acta Cryst.* **E66**, o2687.
- Lobana, T. S., Sharma, R., Bawa, G. & Khanna, S. (2009). *Coord. Chem. Rev.* **253**, 977–1055.
- Oliveira, A. B. de, Beck, J., Landvogt, C., Farias, R. L. de & Feitoza, B. R. S. (2017). *Acta Cryst.* **E73**, 291–295.
- Palve, A. M. & Garje, S. S. (2011). *J. Cryst. Growth*, **326**, 157–162.
- Parrilha, G. L., dos Santos, R. G. & Beraldo, H. (2022). *Coord. Chem. Rev.* **458**, 214418.
- Pawar, A. S. & Garje, S. S. (2015). *Bull. Mater. Sci.* **38**, 1843–1850.
- Pawar, A. S., Masikane, S. C., Mlowe, S., Garje, S. S. & Revaprasadu, N. (2016). *Eur. J. Inorg. Chem.* **2016**, 366–372.
- Rocha, F. V., Farias, R. L., Lima, M. A., Batista, V. S., Nascimento-Júnior, N. M., Garrido, S. S., Leopoldino, A. M., Goto, R. N., Oliveira, A. B., Beck, J., Landvogt, C., Mauro, A. E. & Netto, A. V. G. (2019). *J. Inorg. Biochem.* **199**, 110725.
- Sheldrick, G. M. (2015a). *Acta Cryst.* **A71**, 3–8.
- Sheldrick, G. M. (2015b). *Acta Cryst.* **C71**, 3–8.
- Silva, Á. R. L. & Martínez-Huitle, C. A. (2021). *J. Mol. Liq.* **343**, 117660.
- Siqueira, L. R. P. de, de Moraes Gomes, P. A. T., de Lima Ferreira, L. P., de Melo Rêgo, M. J. B. & Leite, A. C. L. (2019). *Eur. J. Med. Chem.* **170**, 237–260.
- Westrip, S. P. (2010). *J. Appl. Cryst.* **43**, 920–925.
- Wolff, S. K., Grimwood, D. J., McKinnon, J. J., Turner, M. J., Jayatilaka, D. & Spackman, M. A. (2012). *Crystal Explorer 3.1*. University of Western Australia, Perth, Australia.

full crystallographic data

IUCrData (2023). **8**, x231020 [https://doi.org/10.1107/S2414314623010209]

2-{1-[(6*R*,*S*)-3,5,5,6,8,8-Hexamethyl-5,6,7,8-tetrahydronaphthalen-2-yl]ethylidene}-*N*-methylhydrazinecarbothioamide

Ana Paula Lopes de Melo, Alex Fabiani Claro Flores, Leandro Bresolin, Bárbara Tirloni and Adriano Bof de Oliveira

2-{1-[(6*R*,*S*)-3,5,5,6,8,8-Hexamethyl-5,6,7,8-tetrahydronaphthalen-2-yl]ethylidene}-*N*-methylhydrazinecarbothioamide

Crystal data

$C_{20}H_{31}N_3S$

$M_r = 345.54$

Monoclinic, $P2_1/c$

$a = 5.867$ (3) Å

$b = 11.790$ (4) Å

$c = 27.983$ (9) Å

$\beta = 94.907$ (14)°

$V = 1928.7$ (12) Å³

$Z = 4$

$F(000) = 752$

$D_x = 1.190$ Mg m⁻³

Mo $K\alpha$ radiation, $\lambda = 0.71073$ Å

Cell parameters from 9284 reflections

$\theta = 2.3$ – 28.0°

$\mu = 0.17$ mm⁻¹

$T = 100$ K

Block, colorless

$0.21 \times 0.20 \times 0.15$ mm

Data collection

Bruker D8 Venture Photon 100 area detector diffractometer

Radiation source: microfocus X-ray tube,

Bruker D8 Venture

φ and ω scans

Absorption correction: multi-scan

(SADABS; Krause *et al.*, 2015)

$T_{\min} = 0.690$, $T_{\max} = 0.746$

31284 measured reflections

4822 independent reflections

3250 reflections with $I > 2\sigma(I)$

$R_{\text{int}} = 0.092$

$\theta_{\max} = 28.4^\circ$, $\theta_{\min} = 2.3^\circ$

$h = -7 \rightarrow 7$

$k = -15 \rightarrow 15$

$l = -37 \rightarrow 34$

Refinement

Refinement on F^2

Least-squares matrix: full

$R[F^2 > 2\sigma(F^2)] = 0.079$

$wR(F^2) = 0.201$

$S = 1.06$

4822 reflections

243 parameters

0 restraints

Primary atom site location: structure-invariant direct methods

Hydrogen site location: inferred from neighbouring sites

H-atom parameters constrained

$w = 1/[\sigma^2(F_o^2) + (0.0692P)^2 + 4.1581P]$

where $P = (F_o^2 + 2F_c^2)/3$

$(\Delta/\sigma)_{\max} < 0.001$

$\Delta\rho_{\max} = 0.70$ e Å⁻³

$\Delta\rho_{\min} = -0.43$ e Å⁻³

Special details

Geometry. All esds (except the esd in the dihedral angle between two l.s. planes) are estimated using the full covariance matrix. The cell esds are taken into account individually in the estimation of esds in distances, angles and torsion angles; correlations between esds in cell parameters are only used when they are defined by crystal symmetry. An approximate (isotropic) treatment of cell esds is used for estimating esds involving l.s. planes.

Fractional atomic coordinates and isotropic or equivalent isotropic displacement parameters (\AA^2)

	<i>x</i>	<i>y</i>	<i>z</i>	$U_{\text{iso}}^*/U_{\text{eq}}$	Occ. (<1)
C1	0.4228 (6)	0.8742 (3)	0.34890 (11)	0.0297 (7)	
H1A	0.317178	0.837602	0.325720	0.044*	
H1B	0.572363	0.874803	0.337439	0.044*	
H1C	0.373714	0.950678	0.353735	0.044*	
C2	0.2556 (5)	0.8079 (2)	0.42119 (10)	0.0201 (6)	
C3	0.5694 (5)	0.6639 (2)	0.51451 (10)	0.0189 (6)	
C4	0.7938 (5)	0.6024 (3)	0.52273 (11)	0.0246 (7)	
H4A	0.767666	0.527218	0.534209	0.037*	
H4B	0.892159	0.642732	0.546098	0.037*	
H4C	0.864955	0.598124	0.493142	0.037*	
C5	0.4408 (5)	0.6874 (2)	0.55703 (10)	0.0174 (6)	
C6	0.3814 (5)	0.5991 (2)	0.58617 (10)	0.0173 (6)	
H6	0.420807	0.525634	0.578021	0.021*	
C7	0.2647 (5)	0.6151 (2)	0.62739 (10)	0.0161 (6)	
C8	0.2060 (5)	0.5121 (2)	0.65701 (10)	0.0198 (6)	
C9A	0.1338 (12)	0.5514 (4)	0.7065 (2)	0.0204 (15)	0.667 (13)
H9A1	0.067164	0.487592	0.722261	0.025*	0.667 (13)
H9A2	0.269015	0.575048	0.726400	0.025*	0.667 (13)
C10A	-0.0367 (13)	0.6481 (4)	0.7029 (2)	0.0188 (13)	0.667 (13)
H10A	-0.165910	0.626313	0.680229	0.023*	0.667 (13)
C9B	0.018 (2)	0.5468 (8)	0.6880 (4)	0.022 (3)	0.333 (13)
H9B1	-0.011379	0.484838	0.709389	0.026*	0.333 (13)
H9B2	-0.121129	0.560822	0.667565	0.026*	0.333 (13)
C10B	0.079 (3)	0.6527 (9)	0.7176 (4)	0.021 (3)	0.333 (13)
H10B	0.227432	0.644511	0.736163	0.025*	0.333 (13)
C18	-0.1252 (7)	0.6661 (3)	0.75207 (12)	0.0351 (9)	
H18A	-0.233592	0.727213	0.750333	0.053*	0.667 (13)
H18B	-0.198066	0.597947	0.761783	0.053*	0.667 (13)
H18C	0.000513	0.684304	0.775024	0.053*	0.667 (13)
H18D	-0.098157	0.731769	0.772011	0.053*	0.333 (13)
H18E	-0.267837	0.674553	0.732900	0.053*	0.333 (13)
H18F	-0.131339	0.599834	0.771876	0.053*	0.333 (13)
C11	0.0770 (5)	0.7569 (2)	0.68317 (10)	0.0206 (6)	
C12	0.2048 (5)	0.7260 (2)	0.63909 (10)	0.0181 (6)	
C13	0.2671 (5)	0.8150 (2)	0.60974 (10)	0.0211 (6)	
H13	0.226173	0.888377	0.617683	0.025*	
C14	0.3863 (5)	0.7999 (2)	0.56956 (11)	0.0208 (6)	
C15	0.4612 (6)	0.9020 (3)	0.54276 (12)	0.0299 (7)	
H15A	0.574184	0.879635	0.521721	0.045*	

H15B	0.525624	0.957293	0.565178	0.045*
H15C	0.331752	0.934086	0.524249	0.045*
C16	0.4184 (6)	0.4431 (3)	0.67218 (16)	0.0464 (11)
H16A	0.484691	0.415578	0.644208	0.070*
H16B	0.377618	0.380093	0.691427	0.070*
H16C	0.527303	0.490084	0.690511	0.070*
C17	0.0399 (8)	0.4351 (3)	0.62847 (14)	0.0493 (11)
H17A	-0.096516	0.476586	0.618334	0.074*
H17B	0.001698	0.372212	0.648087	0.074*
H17C	0.108789	0.407383	0.600831	0.074*
C19	0.2376 (7)	0.8235 (4)	0.71795 (14)	0.0469 (11)
H19A	0.160960	0.842218	0.745876	0.070*
H19B	0.282993	0.891975	0.702797	0.070*
H19C	0.370519	0.778582	0.727203	0.070*
C20	-0.1305 (6)	0.8300 (4)	0.66802 (14)	0.0421 (10)
H20A	-0.235503	0.787662	0.646723	0.063*
H20B	-0.082284	0.896632	0.651908	0.063*
H20C	-0.204601	0.851976	0.695883	0.063*
N1	0.4303 (4)	0.8132 (2)	0.39367 (9)	0.0217 (5)
H1	0.554520	0.778200	0.403201	0.026*
N2	0.2951 (4)	0.7419 (2)	0.46157 (9)	0.0215 (5)
H2	0.190095	0.733073	0.480892	0.026*
N3	0.5059 (4)	0.6897 (2)	0.47075 (9)	0.0196 (5)
S1	0.00559 (14)	0.87428 (7)	0.41079 (3)	0.0293 (2)

Atomic displacement parameters (Å²)

	U^{11}	U^{22}	U^{33}	U^{12}	U^{13}	U^{23}
C1	0.0322 (18)	0.0341 (18)	0.0226 (15)	0.0026 (15)	0.0019 (13)	0.0073 (14)
C2	0.0222 (15)	0.0177 (14)	0.0199 (14)	-0.0027 (11)	-0.0006 (12)	-0.0013 (11)
C3	0.0199 (15)	0.0181 (13)	0.0190 (14)	-0.0023 (11)	0.0039 (11)	0.0011 (11)
C4	0.0213 (16)	0.0292 (16)	0.0237 (15)	0.0049 (12)	0.0040 (12)	0.0034 (12)
C5	0.0164 (14)	0.0200 (14)	0.0161 (13)	-0.0018 (11)	0.0022 (11)	-0.0005 (11)
C6	0.0192 (15)	0.0127 (12)	0.0203 (14)	0.0017 (10)	0.0028 (11)	0.0001 (10)
C7	0.0161 (14)	0.0136 (12)	0.0182 (13)	0.0002 (10)	-0.0006 (11)	0.0024 (10)
C8	0.0246 (16)	0.0156 (13)	0.0198 (14)	0.0001 (11)	0.0057 (12)	0.0013 (11)
C9A	0.029 (3)	0.016 (2)	0.016 (3)	-0.002 (2)	0.005 (2)	-0.0001 (18)
C10A	0.021 (3)	0.023 (2)	0.013 (2)	0.005 (2)	0.002 (2)	-0.0004 (18)
C9B	0.026 (7)	0.024 (5)	0.015 (5)	-0.003 (4)	0.001 (5)	-0.004 (4)
C10B	0.019 (6)	0.033 (5)	0.011 (5)	0.007 (4)	0.001 (4)	0.003 (4)
C18	0.052 (2)	0.0295 (17)	0.0265 (17)	0.0067 (16)	0.0211 (16)	0.0024 (14)
C11	0.0246 (16)	0.0169 (13)	0.0207 (14)	0.0022 (12)	0.0040 (12)	-0.0011 (11)
C12	0.0205 (15)	0.0160 (13)	0.0174 (14)	-0.0003 (11)	-0.0013 (11)	-0.0019 (10)
C13	0.0270 (16)	0.0141 (13)	0.0223 (15)	0.0009 (11)	0.0020 (12)	0.0004 (11)
C14	0.0233 (16)	0.0173 (13)	0.0218 (15)	-0.0020 (12)	0.0028 (12)	0.0014 (11)
C15	0.045 (2)	0.0150 (14)	0.0304 (17)	-0.0027 (13)	0.0087 (15)	0.0030 (12)
C16	0.033 (2)	0.037 (2)	0.069 (3)	-0.0020 (16)	-0.0022 (19)	0.035 (2)
C17	0.063 (3)	0.041 (2)	0.040 (2)	-0.033 (2)	-0.0184 (19)	0.0190 (18)

C19	0.030 (2)	0.070 (3)	0.041 (2)	-0.0010 (19)	0.0093 (17)	-0.035 (2)
C20	0.029 (2)	0.067 (3)	0.0313 (19)	0.0194 (18)	0.0073 (15)	0.0040 (18)
N1	0.0247 (14)	0.0228 (13)	0.0179 (12)	0.0035 (10)	0.0030 (10)	0.0038 (10)
N2	0.0180 (13)	0.0256 (13)	0.0214 (13)	0.0030 (10)	0.0038 (10)	0.0040 (10)
N3	0.0180 (13)	0.0214 (12)	0.0193 (12)	0.0002 (10)	0.0009 (10)	0.0022 (10)
S1	0.0228 (4)	0.0270 (4)	0.0376 (5)	0.0034 (3)	0.0002 (3)	0.0079 (3)

Geometric parameters (Å, °)

C1—N1	1.442 (4)	C10B—C18	1.609 (11)
C1—H1A	0.9600	C10B—H10B	0.9800
C1—H1B	0.9600	C18—H18A	0.9600
C1—H1C	0.9600	C18—H18B	0.9600
C2—N1	1.335 (4)	C18—H18C	0.9600
C2—N2	1.376 (4)	C18—H18D	0.9600
C2—S1	1.666 (3)	C18—H18E	0.9600
C3—N3	1.286 (4)	C18—H18F	0.9600
C3—C5	1.489 (4)	C11—C19	1.515 (5)
C3—C4	1.503 (4)	C11—C20	1.523 (5)
C4—H4A	0.9600	C11—C12	1.541 (4)
C4—H4B	0.9600	C12—C13	1.400 (4)
C4—H4C	0.9600	C13—C14	1.386 (4)
C5—C6	1.385 (4)	C13—H13	0.9300
C5—C14	1.416 (4)	C14—C15	1.503 (4)
C6—C7	1.403 (4)	C15—H15A	0.9600
C6—H6	0.9300	C15—H15B	0.9600
C7—C12	1.400 (4)	C15—H15C	0.9600
C7—C8	1.526 (4)	C16—H16A	0.9600
C8—C17	1.510 (5)	C16—H16B	0.9600
C8—C9B	1.515 (10)	C16—H16C	0.9600
C8—C16	1.518 (5)	C17—H17A	0.9600
C8—C9A	1.554 (5)	C17—H17B	0.9600
C9A—C10A	1.515 (9)	C17—H17C	0.9600
C9A—H9A1	0.9700	C19—H19A	0.9600
C9A—H9A2	0.9700	C19—H19B	0.9600
C10A—C18	1.527 (5)	C19—H19C	0.9600
C10A—C11	1.568 (6)	C20—H20A	0.9600
C10A—H10A	0.9800	C20—H20B	0.9600
C9B—C10B	1.524 (19)	C20—H20C	0.9600
C9B—H9B1	0.9700	N1—H1	0.8600
C9B—H9B2	0.9700	N2—N3	1.386 (3)
C10B—C11	1.560 (10)	N2—H2	0.8600
N1—C1—H1A	109.5	H18A—C18—H18C	109.5
N1—C1—H1B	109.5	H18B—C18—H18C	109.5
H1A—C1—H1B	109.5	C10B—C18—H18D	109.5
N1—C1—H1C	109.5	C10B—C18—H18E	109.5
H1A—C1—H1C	109.5	H18D—C18—H18E	109.5

H1B—C1—H1C	109.5	C10B—C18—H18F	109.5
N1—C2—N2	114.6 (3)	H18D—C18—H18F	109.5
N1—C2—S1	125.8 (2)	H18E—C18—H18F	109.5
N2—C2—S1	119.6 (2)	C19—C11—C20	108.9 (3)
N3—C3—C5	126.3 (3)	C19—C11—C12	108.6 (3)
N3—C3—C4	116.0 (3)	C20—C11—C12	110.1 (3)
C5—C3—C4	117.7 (2)	C19—C11—C10B	92.3 (6)
C3—C4—H4A	109.5	C20—C11—C10B	125.6 (6)
C3—C4—H4B	109.5	C12—C11—C10B	109.2 (4)
H4A—C4—H4B	109.5	C19—C11—C10A	117.3 (4)
C3—C4—H4C	109.5	C20—C11—C10A	102.0 (4)
H4A—C4—H4C	109.5	C12—C11—C10A	109.8 (3)
H4B—C4—H4C	109.5	C7—C12—C13	118.6 (3)
C6—C5—C14	119.0 (2)	C7—C12—C11	123.9 (2)
C6—C5—C3	120.0 (2)	C13—C12—C11	117.5 (2)
C14—C5—C3	120.9 (2)	C14—C13—C12	123.7 (3)
C5—C6—C7	123.2 (3)	C14—C13—H13	118.1
C5—C6—H6	118.4	C12—C13—H13	118.1
C7—C6—H6	118.4	C13—C14—C5	117.5 (3)
C12—C7—C6	117.9 (2)	C13—C14—C15	119.5 (3)
C12—C7—C8	122.9 (2)	C5—C14—C15	123.0 (3)
C6—C7—C8	119.2 (2)	C14—C15—H15A	109.5
C17—C8—C9B	89.8 (6)	C14—C15—H15B	109.5
C17—C8—C16	107.6 (3)	H15A—C15—H15B	109.5
C9B—C8—C16	127.2 (6)	C14—C15—H15C	109.5
C17—C8—C7	110.9 (3)	H15A—C15—H15C	109.5
C9B—C8—C7	107.7 (4)	H15B—C15—H15C	109.5
C16—C8—C7	111.1 (3)	C8—C16—H16A	109.5
C17—C8—C9A	116.0 (4)	C8—C16—H16B	109.5
C16—C8—C9A	101.0 (4)	H16A—C16—H16B	109.5
C7—C8—C9A	109.8 (3)	C8—C16—H16C	109.5
C10A—C9A—C8	113.1 (5)	H16A—C16—H16C	109.5
C10A—C9A—H9A1	109.0	H16B—C16—H16C	109.5
C8—C9A—H9A1	109.0	C8—C17—H17A	109.5
C10A—C9A—H9A2	109.0	C8—C17—H17B	109.5
C8—C9A—H9A2	109.0	H17A—C17—H17B	109.5
H9A1—C9A—H9A2	107.8	C8—C17—H17C	109.5
C9A—C10A—C18	108.5 (5)	H17A—C17—H17C	109.5
C9A—C10A—C11	110.0 (5)	H17B—C17—H17C	109.5
C18—C10A—C11	113.1 (4)	C11—C19—H19A	109.5
C9A—C10A—H10A	108.4	C11—C19—H19B	109.5
C18—C10A—H10A	108.4	H19A—C19—H19B	109.5
C11—C10A—H10A	108.4	C11—C19—H19C	109.5
C8—C9B—C10B	112.6 (11)	H19A—C19—H19C	109.5
C8—C9B—H9B1	109.1	H19B—C19—H19C	109.5
C10B—C9B—H9B1	109.1	C11—C20—H20A	109.5
C8—C9B—H9B2	109.1	C11—C20—H20B	109.5
C10B—C9B—H9B2	109.1	H20A—C20—H20B	109.5

H9B1—C9B—H9B2	107.8	C11—C20—H20C	109.5
C9B—C10B—C11	108.7 (10)	H20A—C20—H20C	109.5
C9B—C10B—C18	104.7 (10)	H20B—C20—H20C	109.5
C11—C10B—C18	109.0 (7)	C2—N1—C1	123.8 (3)
C9B—C10B—H10B	111.4	C2—N1—H1	118.1
C11—C10B—H10B	111.4	C1—N1—H1	118.1
C18—C10B—H10B	111.4	C2—N2—N3	119.3 (2)
C10A—C18—H18A	109.5	C2—N2—H2	120.4
C10A—C18—H18B	109.5	N3—N2—H2	120.4
H18A—C18—H18B	109.5	C3—N3—N2	117.6 (2)
C10A—C18—H18C	109.5		
N3—C3—C5—C6	122.5 (3)	C18—C10A—C11—C19	43.8 (6)
C4—C3—C5—C6	-56.4 (4)	C9A—C10A—C11—C20	163.7 (5)
N3—C3—C5—C14	-60.3 (4)	C18—C10A—C11—C20	-74.9 (5)
C4—C3—C5—C14	120.7 (3)	C9A—C10A—C11—C12	47.0 (6)
C14—C5—C6—C7	1.4 (4)	C18—C10A—C11—C12	168.4 (4)
C3—C5—C6—C7	178.6 (3)	C6—C7—C12—C13	-1.0 (4)
C5—C6—C7—C12	0.5 (4)	C8—C7—C12—C13	179.8 (3)
C5—C6—C7—C8	179.7 (3)	C6—C7—C12—C11	-179.9 (3)
C12—C7—C8—C17	114.7 (4)	C8—C7—C12—C11	0.9 (4)
C6—C7—C8—C17	-64.4 (4)	C19—C11—C12—C7	112.6 (3)
C12—C7—C8—C9B	17.9 (7)	C20—C11—C12—C7	-128.3 (3)
C6—C7—C8—C9B	-161.3 (7)	C10B—C11—C12—C7	13.2 (7)
C12—C7—C8—C16	-125.6 (3)	C10A—C11—C12—C7	-16.9 (5)
C6—C7—C8—C16	55.2 (4)	C19—C11—C12—C13	-66.3 (4)
C12—C7—C8—C9A	-14.8 (5)	C20—C11—C12—C13	52.8 (4)
C6—C7—C8—C9A	166.0 (4)	C10B—C11—C12—C13	-165.6 (7)
C17—C8—C9A—C10A	-79.7 (6)	C10A—C11—C12—C13	164.3 (4)
C16—C8—C9A—C10A	164.3 (5)	C7—C12—C13—C14	-0.2 (5)
C7—C8—C9A—C10A	47.0 (7)	C11—C12—C13—C14	178.7 (3)
C8—C9A—C10A—C18	170.6 (4)	C12—C13—C14—C5	2.0 (5)
C8—C9A—C10A—C11	-65.3 (7)	C12—C13—C14—C15	-175.1 (3)
C17—C8—C9B—C10B	-165.1 (10)	C6—C5—C14—C13	-2.5 (4)
C16—C8—C9B—C10B	82.6 (10)	C3—C5—C14—C13	-179.7 (3)
C7—C8—C9B—C10B	-53.2 (12)	C6—C5—C14—C15	174.5 (3)
C8—C9B—C10B—C11	70.2 (14)	C3—C5—C14—C15	-2.6 (5)
C8—C9B—C10B—C18	-173.3 (6)	N2—C2—N1—C1	177.7 (3)
C9B—C10B—C11—C19	-156.1 (10)	S1—C2—N1—C1	-3.1 (4)
C18—C10B—C11—C19	90.3 (8)	N1—C2—N2—N3	1.2 (4)
C9B—C10B—C11—C20	88.6 (9)	S1—C2—N2—N3	-178.1 (2)
C18—C10B—C11—C20	-25.0 (12)	C5—C3—N3—N2	-1.8 (4)
C9B—C10B—C11—C12	-45.5 (12)	C4—C3—N3—N2	177.2 (2)
C18—C10B—C11—C12	-159.1 (6)	C2—N2—N3—C3	155.7 (3)
C9A—C10A—C11—C19	-77.6 (5)		

Hydrogen-bond geometry (Å, °)

<i>D—H⋯A</i>	<i>D—H</i>	<i>H⋯A</i>	<i>D⋯A</i>	<i>D—H⋯A</i>
N1—H1⋯S1 ⁱ	0.86	2.87	3.445 (3)	126

Symmetry code: (i) $x+1, y, z$.